Structural Engineering and Mechanics, Vol. 13, No. 6 (2002) 695-711
DOI: http://dx.doi.org/10.12989/sem.2002.13.6.695

Comparative dynamic studies of thick laminated composite shells based on higher-order theories

M. Ganapathi†, B. P. Patel‡, D. S. Pawargi‡† and H. G. Patel‡†

Institute of Armament Technology, Girinagar, Pune-411 025, India

(Received November 19, 2001, Accepted March 5, 2002)

Abstract. Here, the dynamic response characteristics of thick cross-ply laminated composite cylindrical shells are studied using a higher-order displacement model. The formulation accounts for the nonlinear variation of the in-plane and transverse displacements through the thickness, and abrupt discontinuity in slope of the in-plane displacements at any interface. The effect of inplane and rotary inertia terms is included. The analysis is carried out using finite element approach. The influences of various terms in the higher-order displacement field on the free vibrations, and transient dynamic response characteristics of cylindrical composite shells subjected to thermal and mechanical loads are analyzed.

Key words: laminated shell; cross-ply; free vibration; transient response; higher-order; finite element; panels.

1. Introduction

The field of aerospace and civil engineering has brought out the significance of analyzing heat resisting, light-weighted structures. The increased use of composite materials in high temperature environment, high strength and stiffness applications have made the mechanical/thermal analysis of composite structures necessary. Laminated fiber reinforced composites are characterized by low transverse shear modulus compared to the in-plane Young's moduli and therefore the classical theory of non-deformable normals based on neglecting transverse shear strains is not acceptable for laminated composite structures.

To account for shear deformation effects, various structural theories proposed for the analysis of composite laminates have been reviewed and assessed in the literature (Noor and Burton 1990, Reddy 1990, Mallikarjuna and Kant 1993). It is brought out that the first-order theory is quite accurate for the estimation of global behaviors like deflection, fundamental frequency and buckling load of composite laminates, but is inadequate for the estimation of higher-order frequencies, mode shapes, large deflections and distribution of stresses. Furthermore, it requires an arbitrary shear correction to the transverse shear stiffness. This has necessitated the introduction of higher-order function in the displacement model based on global approach, and layer-wise theory for the study of plates/shells

† Professor
‡ Scientist
‡† Graduate Student

(Lo *et al*. 1977, Lee *et al*. 1990, Khdeir and Reddy 1999, Cho *et al*. 1991, Chang and Huang 1991, Tenneti and Chandrashekhara 1994, Xavier *et al*. 1993, Di Sciuva and Icardi 1993, He 1994, Shu and Sun 1994, Icardi 1998, Ossadzow *et al.* 1999, Makhecha *et al.* 2001). In all the laminated plate work concerning global approach, the zig-zag theory with/without through thickness variation in transverse displacement is introduced in the kinematics. It is further noticed from the literature that the contribution of various terms involved in the higher-order displacement kinematics is studied for the static and dynamic characteristics of thick laminated plates (Kant and Swaminathan 2001, Carrera and Krause 1998, Ganapathi and Makhecha 2001, Makhecha *et al.* 2001) whereas such studies for the shell analysis are rather limited. Also, the application of higher-order formulation for dynamic analysis of composite shells, in particular, due to different loading environment is scarce in the literature. Recently, based on exact elasticity analysis of laminated composite plates (Bhaskar *et al.* 1996), an improved kinematics for higher order theory has been suggested for laminated plates by combining zig-zag theory along with variable transverse displacement across the thickness (Ali *et al.* 1999) for the accurate results. But the analysis of composite shells has been carried out using higher-order displacement model having zig-zag function along with constant transverse displacement (Bhaskar and Varadan 1991, Xavier *et al*. 1993, Icardi 1998) while studying the static responses due to pressure load. However, the use of refined kinematics, including zig-zag theory and variable transverse displacement across the thickness for higher-order model seems to be scarce in the literature for the analysis of laminated thick shells.

Here, employing a higher-order theory with zig-zag function along with variable transverse displacement, the dynamic analysis is carried out by extending the finite element approach of Makhecha *et al.* (2001) for studying the free vibration characteristics and forced response behavior of cross-ply cylindrical shells subjected to thermal/mechanical loads. All the inertia terms, due to the parts resulting from first-order model, the higher order displacement function, and the coupling between the different order displacement are included in evaluating the kinetic energy. Frequency values are obtained through eigenvalue analysis and the response characteristics are evaluated using Newmark integration technique. The numerical results evaluated here illustrate not only the significance of the present model but also highlight the comparative study of the response characteristics of laminated composite shell structure, predicted by the different possible higher-order structural models.

2. Formulation

A laminated composite shell of revolution is considered with the co-ordinates x along the meridional direction, y along the circumferential direction and z along the thickness direction having origin at the mid-plane of the shell. Based on Taylor's series expansion method for deducing the two-dimensional formulation of a three-dimensional elasticity problem, the in-plane displacements u^k and v^k, and the transverse displacement w^k for the kth layer, are assumed as (Ali *et al*. 1999, Ganapathi and Makhecha 2001)

$$u^k(x, y, z, t) = u_0(x, y, t) + z\theta_x(x, y, t) + z^2\beta_x(x, y, t) + z^3\phi_x(x, y, t) + S^k\psi_x(x, y, t)$$
$$v^k(x, y, z, t) = v_0(x, y, t) + z\theta_y(x, y, t) + z^2\beta_y(x, y, t) + z^3\phi_y(x, y, t) + S^k\psi_y(x, y, t)$$
$$w^k(x, y, z, t) = w_0(x, y, t) + zw_1(x, y, t) + z^2\Gamma(x, y, t) \quad (1)$$

where t is the time.

The terms with even power in z in the in-plane displacements and those odd in z occurring in the expansion for w^k correspond to stretching problems. But, the terms with odd in z in the in-plane displacements and those even in z in the expression for w^k represent the flexure problems. u_0, v_0, w_0 are the displacements of a generic point on the reference surface; θ_x, θ_y are the rotations of normal to the reference surface about the y and x axes, respectively; w_1, β_x, β_y, Γ, ϕ_x, ϕ_y are the higher order terms in the Taylor's series expansions, defined at the reference surface. ψ_x and ψ_y are generalized variables associated with the zig-zag function, S^k.

The zig-zag function, S^k, as given in the work of Murukami (1986), is defined by

$$S^k = 2(-1)^k z_k / h_k \tag{2}$$

where z_k is the local transverse coordinate with its origin at the centre of the kth layer and h_k is the corresponding layer thickness. Thus, the zig-zag function is piecewise linear with values of −1 and 1 alternately at the different interfaces. The 'zig-zag' function, as defined above, takes care of inclusion of the slope discontinuity of u and v at the interfaces of the laminate as observed in exact three-dimensional elasticity solutions of thick laminated composite structures. The use of such function is more economical than a discrete layer approach of approximating the displacement variations over the thickness of each layer separately. Although both these approaches account for slope discontinuity at the interfaces, in the discrete layer approach the number of unknowns increases with the increase in the number of layers, whereas it remains constant in the present approach.

The strains in terms of mid-plane deformation, rotations of normal, and higher order terms associated with displacements for kth layer are as,

$$\{\varepsilon\} = \begin{Bmatrix} \varepsilon_{bm} \\ \varepsilon_s \end{Bmatrix} - \{\bar{\varepsilon}_t\} \tag{3}$$

The vector $\{\varepsilon_{bm}\}$ includes the bending and membrane terms of the strain components and vector $\{\varepsilon_s\}$ contains the transverse shear strain terms. These strain vectors can be defined as (Kraus 1967)

$$\begin{Bmatrix} \varepsilon_{bm} \\ \varepsilon_s \end{Bmatrix} = \begin{Bmatrix} \varepsilon_{xx} \\ \varepsilon_{yy} \\ \varepsilon_{zz} \\ \varepsilon_{xy} \\ \varepsilon_{xz} \\ \varepsilon_{yz} \end{Bmatrix} = \begin{Bmatrix} (u^k_{,x} + w/R_1)/(1 + z/R_1) \\ (v^k, y + (u^k/r)\cos\phi + (w^k/r)\sin\phi)/(1 + z/R_2) \\ w^k, z \\ (u^k_{,y} - (v^k/r)\cos\phi)/(1 + z/R_2) + v^k_{,x}/(1 + z/R_1) \\ u^k_{,z} + (w^k_{,x} - u/R_1)/(1 + z/R_1) \\ v^k_{,z} + (w^k_{,y} - (v/r)\sin\phi)/(1 + z/R_2) \end{Bmatrix} \tag{4}$$

where R_1, R_2 are the principal radii of curvature in meridional and hoop directions, respectively; r is the radius of the parallel circle; and ϕ is the angle between normal and axis of revolution.

The subscript comma denotes the partial derivative with respect to the spatial coordinate succeeding it.

Using the kinematics given in Eq. (1), Eq. (4) can be rewritten as

$$\begin{Bmatrix} \varepsilon_{bm} \\ \varepsilon_s \end{Bmatrix} = [\bar{Z}]\{\varepsilon_1 \ \varepsilon_2 \ \varepsilon_3 \ \varepsilon_4 \ \varepsilon_5 \ \varepsilon_6 \ \varepsilon_7 \ \varepsilon_8 \ \varepsilon_9 \ \varepsilon_{10} \ \varepsilon_{11} \ \varepsilon_{12} \ \varepsilon_{13} \ \varepsilon_{14}\}^T \tag{5a}$$

where

$$[\bar{Z}] = \begin{bmatrix} Z_1 & Z_2 & Z_3 & Z_4 & Z_5 & O_1 & O_1 & O_1 & O_1 & O_1 & O_1 & O_1 & O_1 & O_1 \\ O_2 & O_2 & O_3 & O_3 & O_3 & Z_6 & Z_7 & Z_8 & Z_9 & Z_{10} & Z_{11} & Z_{12} & Z_{13} & Z_{14} \end{bmatrix} \tag{5b}$$

The various submatrices involved in Eq. (5) are given in Appendix A.

The thermal strain vector $\{\bar{\varepsilon}_t\}$ is represented as

$$\{\bar{\varepsilon}_t\} = \begin{Bmatrix} \bar{\varepsilon}_{xx} \\ \bar{\varepsilon}_{yy} \\ \bar{\varepsilon}_{zz} \\ \bar{\varepsilon}_{xy} \\ \bar{\varepsilon}_{xz} \\ \bar{\varepsilon}_{yz} \end{Bmatrix} = \Delta T \begin{Bmatrix} \alpha_x \\ \alpha_y \\ \alpha_z \\ \alpha_{xy} \\ 0 \\ 0 \end{Bmatrix} \tag{6}$$

where ΔT is the rise in temperature and is generally represented as function of x, y, and z. α_x, α_y, α_z and α_{xy} are thermal expansion coefficients in the shell coordinates and can be related to to the thermal expansion coefficients (α_1, α_2 and α_3) in the material principal directions.

The constitutive relations for an arbitary layer k, in the laminated shell (x, y, z) coordinate system can be expressed as

$$\{\sigma\} = \{\sigma_{xx} \ \sigma_{yy} \ \sigma_{zz} \ \tau_{xy} \ \tau_{xz} \ \tau_{yz}\}^T = [\bar{Q}_k]\{\varepsilon_{xx} - \bar{\varepsilon}_{xx} \ \varepsilon_{yy} - \bar{\varepsilon}_{yy} \ \varepsilon_{zz} - \bar{\varepsilon}_{zz} \ \gamma_{xy} - \bar{\gamma}_{xy} \ \gamma_{xz} \ \gamma_{yz}\}^T \tag{7}$$

where the terms of $[\bar{Q}_k]$ matrix of kth ply are referred to the laminated shell axes and can be obtained from the $[Q_k]$ corresponding to the fibre directions with the appropriate transformation, as outlined in the literature (Jones 1975). $\{\alpha\}$, $\{\varepsilon\}$, $\{\bar{\varepsilon}_t\}$ are stress, strain, and thermal strain vectors due to rise in temperature, respectively. The superscript T refers the transpose of a matrix/vector.

The governing equations are obtained by applying Lagrangian equations of motion given by

$$d/dt[\partial(T - U_T)/\partial\dot{\delta}_i] - [\partial(T - U_T)/\partial\delta_i] = 0, \quad i = 1 \text{ to } n \tag{8}$$

where T is the kinetic energy; U_T is the total potential energy consisting of strain energy contributions due to the in-plane and transverse stresses, and work done by the externally applied mechanical loads, respectively. $\{\delta\} = \{\delta_1, \ \delta_2, \cdots, \ \delta_i, \cdots, \ \delta_n\}^T$ is the vector of the degree of freedoms/generalized coordinates. A dot over the variables represents the partial derivative with respect to time.

The kinetic energy of the plate is given by

$$T(\delta) = \frac{1}{2}\iint\left[\sum_{k=1}^{n}\int_{h_k}^{h_{k+1}} \rho_k\{\dot{u}^k \ \dot{v}^k \ \dot{w}^k\}\{\dot{u}^k \ \dot{v}^k \ \dot{w}^k\}^T\left(1 + \frac{z}{R_1}\right)\left(1 + \frac{z}{R_2}\right)dz\right]dxdy \tag{9}$$

where ρ_k is the mass density of the kth layer. h_k, h_{k+1} are the z coordinates of laminate corresponding to the bottom and top surfaces of the kth layer.

Using the kinematics given in Eq. (1), Eq. (9) can be rewritten as

$$T(\delta) = \frac{1}{2}\iint\left[\sum_{k=1}^{n}\int_{h_k}^{h_{k+1}}\rho_k\{\dot{d}^e\}^T[Z]^T[Z]\{\dot{d}^e\}\left(1+\frac{z}{R_1}\right)\left(1+\frac{z}{R_2}\right)dz\right]dxdy \tag{10}$$

where $\{\dot{d}^e\}^T = \{\dot{u}_0\ \dot{v}_0\ \dot{w}_0\ \dot{\theta}_x\ \dot{\theta}_y\ \dot{w}_1\ \dot{\beta}_x\ \dot{\beta}_y\ \dot{\Gamma}\ \dot{\phi}_x\ \dot{\phi}_y\ \dot{\psi}_x\ \dot{\psi}_y\}$ and

$$[Z] = \begin{bmatrix} 1 & 0 & 0 & z & 0 & 0 & z^2 & 0 & 0 & z^3 & 0 & S^k & 0 \\ 0 & 1 & 0 & 0 & z & 0 & 0 & z^2 & 0 & 0 & z^3 & 0 & S^k \\ 0 & 0 & 1 & 0 & 0 & z & 0 & 0 & z^2 & 0 & 0 & 0 & 0 \end{bmatrix}$$

The total potential energy functional U_T consisting of strain energy contributions due to the in-plane and transverse stresses, and work done by the externally applied mechanical loads, is given by,

$$U_T(\delta) = \frac{1}{2}\iint\left[\sum_{k=1}^{n}\int_{h_k}^{h_{k+1}}\{\sigma\}^T\{\varepsilon\}\left(1+\frac{z}{R_1}\right)\left(1+\frac{z}{R_2}\right)dz\right]dxdy + \iint qw\,dxdy \tag{11}$$

where q is the distributed pressure load acting on the middle surface of the shell.

For obtaining the element level governing equations, the kinetic and the total potential energies may be conveniently written as

$$T(\delta^e) = \frac{1}{2}\{\dot{\delta}^e\}^T[M^e][\dot{\delta}^e] \tag{12}$$

$$\begin{aligned} U_T(\delta^e) = {} & \frac{1}{2}\{\delta^e\}^T[K^e]\{\delta^e\} - \{\delta^e\}^T\{F_T^e\} - \{\delta^e\}^T\{F_M^e\} \\ & + \frac{1}{2}\iint\left[\sum_{k=1}^{n}\int_{h_k}^{h_{k+1}}\{\bar{\varepsilon}_t\}^T[\bar{Q}_k]\{\bar{\varepsilon}_t\}\left(1+\frac{z}{R_1}\right)\left(1+\frac{z}{R_2}\right)dz\right]dxdy \end{aligned} \tag{13}$$

The elemental mass and stiffness matrices, and thermal/mechanical load vectors involved in Eqs. (12) and (13) can be defined as

$$[M^e] = \iint\left[\sum_{k=1}^{n}\int_{h_k}^{h_{k+1}}\rho_k\{H\}^T[Z]^T[Z]\{H\}\left(1+\frac{z}{R_1}\right)\left(1+\frac{z}{R_2}\right)dz\right]dxdy \tag{14a}$$

$$[K^e] = \iint\left[\sum_{k=1}^{n}\int_{h_k}^{h_{k+1}}[B]^T[\bar{Z}]^T[\bar{Q}_k][\bar{Z}][B]\left(1+\frac{z}{R_1}\right)\left(1+\frac{z}{R_2}\right)dz\right]dxdy \tag{14b}$$

$$[F_T^e] = \iint\left[\sum_{k=1}^{n}\int_{h_k}^{h_{k+1}}[B]^T[\bar{Z}]^T[\bar{Q}_k]\{\bar{\varepsilon}_t\}\left(1+\frac{z}{R_1}\right)\left(1+\frac{z}{R_2}\right)dz\right]dxdy \tag{14c}$$

$$[F_M^e] = \iint \{H_w\}^T q dx dy \tag{14d}$$

Here $\{\delta^e\}$ is the vector of the elemental degrees of freedoms/generalized coordinates, and $[H]$ and $[B]$ are the interpolation and strain matrices pertaining to the element, respectively.

Substituting Eqs. (12) and (13) in Eq. (8), one obtains the governing equation for the element as,

$$[M^e]\{\ddot{\delta}^e\} + [K^e]\{\delta^e\} = \{F_T^e\} + \{F_M^e\} \tag{15}$$

The coefficients of mass and stiffness matrices, and the load vectors involved in governing Eq. (15) can be rewritten as the product of term having thickness co-ordinate z alone and the term containing x and y. In the present study, while performing the integration, terms having thickness co-ordinate z are explicitly integrated whereas the terms containing x and y are evaluated using full integration with 3×3 points Gauss integration rule.

Following the usual finite element assembly procedure (Zienkiewicz 1971), the governing equation for the forced response of the laminated shell are obtained as

$$[M]\{\ddot{\delta}\} + [K]\{\delta\} = \{F_T\} + \{F_M\} \tag{16}$$

where $[M]$ and $[K]$ are the global mass and stiffness matrices. $\{F_T\}$, $\{F_M\}$ are the global thermal and mechanical load vectors, repectively.

The solutions of Eq. (16) can be obtained using either standard eigenvalue algorithm for free vibration study or employing Newmark's direct integration method for dynamic response analysis.

3. Element description

In the present work, a simple C^0 continous, eight-noded serendipity quadrilateral shear flexible shell element (HSDT13) with thirteen nodal degrees of freedom (u_0, v_0, w_0, θ_x, θ_y, w_1, β_x, β_y, Γ, ϕ_x, ϕ_y, ψ_x and ψ_y : 13-DOF) developed based on field consistency approach (Prathap 1985) is employed.

If the interpolation functions for an eight-noded element are used directly to interpolate the thirteen field variables u_0, … ψ_y in deriving the membrane and shear strains, the element will lock and show oscillation in the membrane and shear stresses. Field consistency requires that the membrane and the transverse shear strains must be interpolated in a consistent manner. Thus, the w_0, and (u_0 and w_0) terms in the expression for membrane strains $\{\varepsilon_1\}$ (first two strain components) given in Eq. (A2) have to be consistent with the field functions $u_{0,x}$ and $v_{0,y}$, respectively. Similarly, the terms (θ_x, u_0) and (θ_y, v_0) in the expression for transverse shear strains ($\{\varepsilon_6\}$ and $\{\varepsilon_{10}\}$) given in Eq. (A3) have to be consistent with the field functions $w_{0,x}$ and $w_{0,y}$, respectively, as outlined in the work of Prathap (1985). This is achieved by using a field-redistributed substitute shape function to interpolate those specific terms that must be consistent. The element thus derived is tested for its basic properties and is found free from the rank deficiency, shear/membrane locking, and poor convergence syndrome (Ganapathi and Makhecha 2001, Makhecha *et al.* 2001).

The finite element represented as per the kinematics given in Eq. (1), is referred as HSDT13 with cubic variation. Five more alternate standard discrete models are proposed, to study the influence of higher order terms in the displacement functions, whose displacement fields are deduced from the original element by deleting the appropriate degrees of freedom (w_1 & $\Gamma = 0$; or $\psi = 0$; or ψ, w_1 & $\Gamma = 0$;

Table 1 Alternate eight-noded finite element models considered for parametric study

Finite element model	Degrees of freedom per node
HSDT13 (Present)	u_0, v_0, w_0, θ_x, θ_y, w_1, β_x, β_y, Γ, ϕ_x, ϕ_y, ψ_x, ψ_y
HSDT11a	u_0, v_0, w_0, θ_x, θ_y, β_x, β_y, ϕ_x, ϕ_y, ψ_x, ψ_y
HSDT11b	u_0, v_0, w_0, θ_x, θ_y, w_1, β_x, β_y, Γ, ϕ_x, ϕ_y
HSDT9	u_0, v_0, w_0, θ_x, θ_y, β_x, β_y, ϕ_x, ϕ_y
HSDT7	u_0, v_0, w_0, θ_x, θ_y, ϕ_x, ϕ_y
FSDT	u_0, v_0, w_0, θ_x, θ_y

or z^2 terms, ψ, w_1 & $\Gamma = 0$; or dropping all the higher-order terms). These alternate models, and the corresponding degrees of freedom are shown in Table 1.

4. Results and discussion

The study, here, has been focussed on the dynamic behavior of laminated composite shells based on higher-order model and also bringing out the influences of various terms assumed in the kinematics on the response characteristics. Although the formulation presented here is general, the analysis is carried out for the free vibration, and the transient responses of cross-ply simply supported cylindrical shells subjected to thermal/mechanical loads. Since the higher-order theory, in general, is required for the accurate analysis of thick composite structures, the emphasis in the present work is placed on the laminated thick shells for the numerical study.

Based on progressive mesh refinement, a 16×8 grid mesh (circumferential and meridional directions) is found to be adequate to model the one-eighth /one-fourth of the closed/open shells for the present analysis. Before proceeding for the detailed study, the formulation developed herein is tested against available three-dimensional elasticity solutions. For the free vibration of laminated plates, the fundamental frequencies are obtained employing various models given in Table 1 and using the conditions $1/R_1 = 1/R_2 = 0$, and they are compared with three-dimensional elasticity solution (Noor 1973) in Table 2 for different orthotropicity values. The results evaluated here for laminated cross-ply cylindrical panels, and circular cylindrical shells are shown in Tables 3 and 4 along with three-dimensional solutions (Bhimaraddi 1991, Ye and Soldatos 1997). It can be seen from Table 2 that, for higher modular ratio E_1/E_2, the present model HSDT13 and HSDT11a predict results very close to those of three-dimensional one. For the cylindrical panel case, the difference in results predicted among various higher-order models is less in comparison with those of three-dimensional FEM (Table 3). However, a noticeable difference is seen between the present results and analytical solutions (Bhimaraddi 1991). This may be attributed to the assumption of $z/R << 1$ involved in the work of Bhimaraddi (1991) whereas no such assumption is used in the present work. The material properties used, unless otherwise mentioned, are

$E_1/E_2 = 40$, $G_{12}/E_2 = G_{13}/E_2 = 0.6$, $G_{23}/E_2 = 0.5$, $\nu_{12} = \nu_{23} = \nu_{13} = 0.25$, $\alpha_2/\alpha_1 = \alpha_3/\alpha_1 = 1125$,
$E_2 = E_3 = 10^9$ N/m^2, $\alpha_1 = 10^{-5}$/°C, $\rho = 1500$ kg/m^3

where E, G and ν are Young's modulus, shear modulus and Poisson's ratio. The subscripts 1, 2, and 3 refer to the principal material directions.

Table 2 Non-dimensional fundamental frequencies ($\overline{\omega} = \omega\sqrt{\rho h^2/E_2} \times 10$) of simply supported cross-ply $(0^o/90^o)_{N/2}$ square plates with $L/h = 5$ ($G_{12}/E_1 = 0.6$, $G_{23}/E_2 = 0.5$, $\nu_{12} = \nu_{13} = \nu_{23} = 0.25$, $E_2 = E_3$)

No. of layers, N	Model	E_1/E_2				
		3	10	20	30	40
2	HSDT13	2.4935	2.7886	3.0778	3.2940	3.4638
	HSDT11a	2.5478	2.7830	3.1066	3.2897	3.4598
	HSDT11b	2.4937	2.7899	3.0858	3.3113	3.4911
	HSDT9	2.5480	2.7843	3.1142	3.3069	3.4870
	HSDT7	2.5177	2.8156	3.1125	3.3391	3.5203
	FSDT5	2.4824	2.7742	3.0802	3.3256	3.5299
	Elasticity* (Noor 1973)	2.5031	2.7938	3.0698	3.2705	3.4250
4	HSDT13	2.6029	3.2488	3.7677	4.0841	4.3001
	HSDT11a	2.6547	3.2408	3.7796	4.0771	4.2936
	HSDT11b	2.6061	3.2595	3.7872	4.1095	4.3290
	HSDT9	2.6580	3.2514	3.7990	4.1023	4.3225
	HSDT7	2.6405	3.3506	3.9521	4.3349	4.6042
	FSDT5	2.6004	3.2871	3.8706	4.2415	4.5007
	Elasticity (Noor 1973)	2.6182	3.2578	3.7622	4.0660	4.2719
6	HSDT13	2.6264	3.3478	3.9219	4.2686	4.5035
	HSDT11a	2.6780	3.3399	3.9321	4.2621	4.4976
	HSDT11b	2.6289	3.3547	3.9342	4.2849	4.5225
	HSDT9	2.6805	3.3468	3.9445	4.2783	4.5166
	HSDT7	2.6630	3.4443	4.0957	4.5053	4.7987
	FSDT5	2.6215	3.3643	3.9719	4.3462	4.6029
	Elasticity (Noor 1973)	2.6440	3.3657	3.9359	4.2783	4.5091
10	HSDT13	2.6390	3.4018	4.0093	4.3770	4.6279
	HSDT11a	2.6905	3.3941	4.0189	4.3709	4.6224
	HSDT11b	2.6410	3.4068	4.0177	4.3881	4.6415
	HSDT9	2.6926	3.3990	4.0274	4.3819	4.6359
	HSDT7	2.6747	3.4926	4.1694	4.5924	4.8671
	FSDT5	2.6321	3.4022	4.0201	4.3952	4.6508
	Elasticity (Noor 1973)	2.6583	3.4250	4.0337	4.4011	4.6498

*Based on higher-order difference scheme

All the layers are of equal thickness and the ply-angle is measured with respect to the x-axis (meridional axis). The simply supported boundary conditions considered here are:

circular cylindrical shell:

$$v_0 = w_0 = \theta_y = w_1 = \Gamma = \beta_y = \phi_y = \psi_y = 0 \text{ at } x = 0, L$$

cylindrical shell panel :

$$v_0 = w_0 = \theta_y = w_1 = \Gamma = \beta_y = \phi_y = \psi_y = 0 \text{ at } x = 0, L$$
$$u_0 = w_0 = \theta_x = w_1 = \Gamma = \beta_x = \phi_x = \psi_x = 0 \text{ at } y = 0, b$$

Table 3 Comparison of natural frequency parameter Ω^{**} (= $\omega L\sqrt{\rho/E_2}$) of a two-layered cross-ply ($90^o/0^o$) cylindrical panel (E_1/E_2 = 25; G_{12}/E_2 = 0.5, G_{23}/E_2 = 0.2, ν_{12} = 0.25, ν_{31} = 0.03, ν_{23} = 0.4, R/L = 1; Longitudinal mode number, m = 1)

h/L	Circum. Wave No. n	HSDT13	3D FEM[$]	HSDT11a	HSDT11b	HSDT9	HSDT7	FSDT5	Bhimaraddi (1991)
0.05	1	0.8067	0.8061	0.8058	0.8068	0.8059	0.8061	0.8057	0.7868
	2	1.2036	1.1981	1.1997	1.2042	1.2000	1.2027	1.1959	-
	3	2.3507	2.3320	2.3413	2.3526	2.3417	2.3548	2.3246	-
	4	3.8175	3.7770	3.7997	3.8226	3.8003	3.8360	3.7585	-
0.1	1	1.0615	1.0581	1.0578	1.0621	1.0584	1.0593	1.0550	1.0409
	2	2.0669	2.0431	2.0544	2.0683	2.0555	2.0701	2.0316	2.0956
	3	3.7234	3.6607	3.6953	3.7258	3.6966	3.7513	3.6280	3.7949
	4	5.5316	5.4247	5.4866	5.5364	5.4882	5.6027	5.3562	5.6331
0.15	1	1.3244	1.3158	1.3170	1.3255	1.3181	1.3209	1.3073	1.2910
	2	2.6395	2.5958	2.6182	2.6416	2.6201	2.6512	2.5684	-
	3	4.4160	4.3256	4.3776	4.4195	4.3801	4.4430	4.2449	-
	4	6.2359	6.1038	6.1945	6.2457	6.1994	6.3567	5.9860	-

[$] Using ANSYS 5.6, 1997

Table 4 Comparision of natural frequency parameter Ω^{*} (= $\omega R\sqrt{\rho/E_2}$) of a three-layered symmetric cross-ply ($0^o/90^o/0^o$) circular cylindrical shell (E_1/E_2 = 25; L/R = 5; Longitudinal mode number, m = 1)

R/h	Circum. Wave Number, n	HSDT13	HSDT11a	HSDT11b	HSDT9	HSDT7	FSDT5	Ye and Soldatos (1997)
5	1	0.339297	0.339277	0.339298	0.339279	0.339302	0.339317	0.339
	2	0.306985	0.307353	0.307330	0.307703	0.307718	0.308509	0.306
	3	0.594289	0.594269	0.596914	0.596907	0.596956	0.602658	0.591
10	1	0.331522	0.331517	0.331522	0.331517	0.331524	0.331525	0.332
	2	0.224928	0.225046	0.224962	0.225080	0.225088	0.225164	0.225
	3	0.330063	0.330193	0.330461	0.330591	0.330595	0.331413	0.329
20	1	0.329408	0.329406	0.329408	0.329406	0.329408	0.329408	0.329
	2	0.197009	0.197041	0.197012	0.197044	0.197046	0.197052	0.197
	3	0.194639	0.194711	0.194685	0.194756	0.194758	0.194850	0.194

Next, the free vibration characteristics obtained for two- and eight-layered cross-ply cylindrical panels of same meridional and circumferential lengths ($L = b$) with different length-to-radius and radius-to-thickness ratios (L/R = 0.5 & 4; R/h = 5, 10) are presented in Tables 5-8. It is observed from Table 5 that the higher-order model HSDT7 predicts the frequency values $\Omega_{mn}(= \omega_{mn}L^2/h\sqrt{\rho/E_2})$ close to those of first-order one and both models are overestimating the frequency values in comparison with those of complete model HSDT13. It is further noticed from Tables 5-7 that, with the increase in number of layers, HSDT7 highly over predicts the results compared to FSDT5. It is also seen from these Tables that the performances of the models HSDT9 and HSDT11b are nearly

Table 5 Non dimensional frequencies of two- and eight-layered cross-ply cylindrical panel with $R/h = 5$ and $L/R = 0.5$

Lamination	Theory	Non dimensional frequency Ω			
		Ω_{11}	Ω_{12}	Ω_{21}	Ω_{22}
$(0^o/90^o)$	HSDT13	5.6423	10.2463	10.4274	13.6080
	HSDT11a	5.6505	10.2917	10.4186	13.5673
	HSDT11b	5.7224	10.3239	10.4877	13.6865
	HSDT9	5.7304	10.3881	10.4846	13.6435
	HSDT7	5.8216	10.6642	10.7745	14.0310
	FSDT5	5.8748	10.6312	10.7675	13.8938
$(0^o/90^o)_4$	HSDT13	6.7472	11.5403	11.6198	14.9291
	HSDT11a	6.7534	11.5766	11.6148	14.9392
	HSDT11b	6.7701	11.5596	11.6412	14.9531
	HSDT9	6.7763	11.5987	11.6362	14.9630
	HSDT7	7.2914	12.3698	12.3966	15.9163
	FSDT5	6.7972	12.0035	12.1675	15.8423

Table 6 Non dimensional frequencies of two- and eight-layered cross-ply cylindrical panel with $R/h = 10$ and $L/R = 0.5$

Lamination	Theory	Non dimensional frequency Ω			
		Ω_{11}	Ω_{12}	Ω_{21}	Ω_{22}
$(0^o/90^o)$	HSDT13	8.3888	17.0826	17.5530	23.2283
	HSDT11a	8.4078	17.1077	17.5183	23.2100
	HSDT11b	8.4626	17.3266	17.7681	23.5057
	HSDT9	8.4818	17.3644	17.7372	23.4848
	HSDT7	8.5501	17.6350	18.0113	23.9015
	FSDT5	8.5862	17.8598	18.2886	24.0531
$(0^o/90^o)_4$	HSDT13	11.2675	20.8572	21.0695	27.4157
	HSDT11a	11.2746	20.8836	21.0485	27.4023
	HSDT11b	11.3019	20.9255	21.1408	27.5120
	HSDT9	11.3092	20.9549	21.1196	27.4987
	HSDT7	11.9330	22.5078	22.6440	29.6018
	FSDT5	11.4058	21.0366	21.2188	27.5707

comparable but the frequency values are higher than that of present model HSDT13. However, the model HSDT11a, in general, appears to yield accurate results against that of the present complete model for short and thick laminated cylindrical panels. With increase in R/h and L/R, it is depicted from Tables 5 and 8 that the difference in the results predicted among various models is decreased as expected.

Next, the influence of various higher terms or models on the natural frequencies of thick laminated circular cylindrical shells is studied and presented in Table 9. It is observed from Table 9

Table 7 Non dimensional frequencies of two- and eight-layered cross-ply cylindrical panel with R/h = 5 and L/R = 4

Lamination	Theory	Non dimensional frequency Ω			
		Ω_{11}	Ω_{12}	Ω_{21}	Ω_{22}
$(0^o/90^o)$	HSDT13	36.6495	27.7523	74.9204	55.0197
	HSDT11a	36.6525	27.9329	74.9734	55.2278
	HSDT11b	36.6517	27.7844	74.9471	55.0848
	HSDT9	36.6547	27.9676	74.9996	55.2942
	HSDT7	36.6613	27.9958	75.0083	55.3395
	FSDT5	36.6638	27.9790	75.0751	55.4075
$(0^o/90^o)_4$	HSDT13	38.3737	34.3371	80.0384	66.2415
	HSDT11a	38.3675	34.7285	80.0245	66.4824
	HSDT11b	38.3744	34.3554	80.0518	66.2815
	HSDT9	38.3682	34.7489	80.0379	66.5236
	HSDT7	38.3824	35.1131	80.2669	67.2341
	FSDT5	38.3748	34.7926	80.1113	66.6777

Table 8 Non dimensional frequencies of two- and eight-layered cross-ply cylindrical panel with R/h = 10 and L/R =4

Lamination	Theory	Non dimensional frequency Ω			
		Ω_{11}	Ω_{12}	Ω_{21}	Ω_{22}
$(0^o/90^o)$	HSDT13	74.1242	51.7260	149.5746	103.7500
	HSDT11a	74.1319	51.8011	149.6293	103.8577
	HSDT11b	74.1247	51.7312	149.5797	103.7628
	HSDT9	74.1324	51.8067	149.6344	103.8707
	HSDT7	74.1366	51.8193	149.6430	103.8973
	FSDT5	74.1344	51.7587	149.6520	103.8750
$(0^o/90^o)_4$	HSDT13	75.5477	57.1457	153.7974	113.2001
	HSDT11a	75.5413	57.2942	153.7942	113.3145
	HSDT11b	75.5478	57.1507	153.8001	113.2101
	HSDT9	75.5414	57.2995	153.7969	113.3247
	HSDT7	75.5434	57.3859	153.8439	113.4952
	FSDT5	75.5417	57.2624	153.8136	113.3389

that, irrespective of short or long cylinder, model HSDT7 over predicts the frequency values whereas FSDT5 under predicts the results for the short and thick case in comparison with those of complete model HSDT13. The model HSDT9 yields results very close to HSDT11a for long cylinder whereas for short cylinder case its performance is rather close to HSDT11b. Also, the difference in the values, in general, increases with the increase in the circumferential wave number. Furthermore, it is inferred that, for a short cylinder, HSDT11a having zig-zag variation through the thickness for in-plane displacements predicts frequency values very close to complete model

Table 9 Frequency parameter Ω (= $\omega R\sqrt{\rho/E_2}$) of an eight-layered unsymmetric cross-ply $(0^o/90^o)_4$ circular cylindrical shell (Longitudinal mode number, m = 1)

Circum. Wave Number n	Theory	L/R					
		5			0.5		
		R/h			R/h		
		2.5	5	10	2.5	5	10
1	HSDT13	0.352448	0.336093	0.331732	4.503126	4.325594	3.971877
	HSDT11a	0.352408	0.336097	0.331739	4.505317	4.323748	3.970198
	HSDT11b	0.352506	0.336098	0.331733	4.505275	4.332821	3.977382
	HSDT9	0.352466	0.336101	0.331739	4.507904	4.331059	3.975679
	HSDT7	0.352681	0.336118	0.331740	4.583386	4.383107	3.997469
	FSDT5	0.352982	0.336156	0.331744	4.487248	4.355006	3.996548
2	HSDT13	0.758660	0.566201	0.371140	4.387114	4.098246	3.568073
	HSDT11a	0.780684	0.576207	0.373572	4.385639	4.095270	3.566235
	HSDT11b	0.760016	0.567005	0.371324	4.391072	4.108857	3.575911
	HSDT9	0.782316	0.577081	0.373762	4.389799	4.105892	3.574049
	HSDT7	0.793617	0.580614	0.374374	4.500067	4.179835	3.604629
	FSDT5	0.794385	0.581616	0.374551	4.357779	4.139150	3.603539
3	HSDT13	1.527944	1.244130	0.835968	4.531517	4.165393	3.502635
	HSDT11a	1.550800	1.259912	0.841047	4.529267	4.162229	3.501198
	HSDT11b	1.530750	1.247065	0.837028	4.536939	4.177905	3.511649
	HSDT9	1.554175	1.263060	0.842135	4.534688	4.174632	3.510179
	HSDT7	1.587034	1.277661	0.845840	4.660843	4.257282	3.544421
	FSDT5	1.575407	1.279348	0.846796	4.501162	4.212103	3.543059
4	HSDT13	2.307072	1.986646	1.451409	4.829248	4.414821	3.645450
	HSDT11a	2.324346	2.003967	1.458411	4.827397	4.412307	3.644882
	HSDT11b	2.310461	1.992089	1.454149	4.835591	4.428982	3.655415
	HSDT9	2.328520	2.009797	1.461220	4.833681	4.426304	3.654817
	HSDT7	2.385855	2.041247	1.471331	4.973065	4.516423	3.691595
	FSDT5	2.342163	2.038262	1.473214	4.796745	4.468223	3.690103

HSDT13 whereas HSDT11b with thickness variation in transverse displacement is more close to the HSDT13 for long cylinder case.

The transient response analysis is carried out considering eight-layered unsymmetric thick cross-ply shell [L/R = 0.5, R/h = 5; $(0^o/90^o)_4$] subjected to [$T = T_0$ $(2z/h)$ $\sin(\pi x/L)$ $\cos(3\ y/R)$; $T_0 = 1$] and internal pressure load [$q = q_0$ $\sin(\pi x/L)$ $\cos(3\ y/R)$; $q_0 = 50$]. The in-plane displacement v and the transverse displacement w presented here correspond to the (x, y, z) locations of ($L/2$, $\pi R/2$, $h/2$) and ($L/2$, 0, $h/2$), respectively. The variation of the displacements evaluated using different models is described in Fig. 1 for the thermal loading case. It is noticed from Fig. 1 that the responses calculated using FSDT5, HSDT7, HSDT9 and even HSDT11a are very low compared to that of HSDT11b/HSDT13. The amplitudes predicted by HSDT11b/HSDT13 are high and the response shows high frequency oscillations due to the participation of thickness stretch modes. However, it

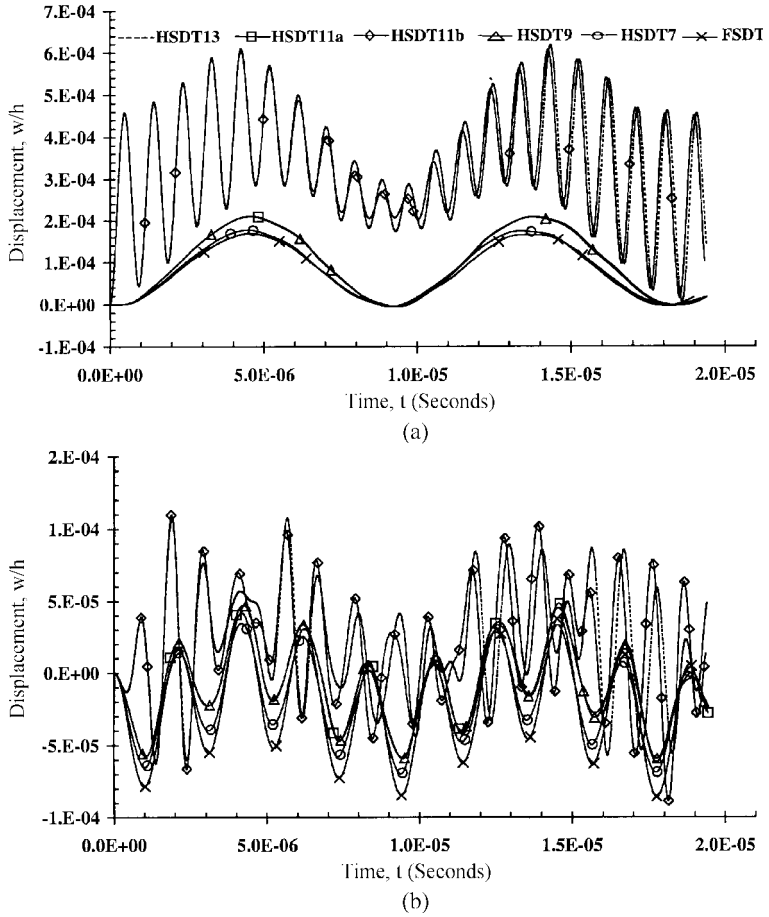

Fig. 1 Transient response of eight-layered unsymmetric cross-ply $(0^o/90^o)_4$ circular cylindrical shell subjected to thermal loading (L/R = 0.5, R/h = 5); (a) w - transverse direction; (b) v-circumferential direction

appears that retaining the thickness stretch terms (w_1 & Γ) in the transverse displacement is more important than the inclusion of zig-zag terms (ψ) in in-plane displacement description.

For the internal pressure load, the transverse and in-plane response characteristics obtained through various models are presented in Fig. 2. It is noticed that the changes in the initial responses predicted by different models are less. However, with the increase in the response time, the variation of displacement depends on the type of models employed. It is further seen that, like thermal case, HSDT9, HSDT7 and FSDT5 predict similar response except the occurrence of peak amplitudes. Although there is some reduction in the maximum amplitude value predicted by HSDT11a, the response pattern is very close to actual model HSDT13 whereas the response period calculated through the model HSDT11b is less in comparison with those of the complete model. In general, it can be opined that, for the mechanical load, the response predicted by the model having zig-zag variation in the in-plane displacement (HSDT11a) is, qualitatively, similar as that of complete model.

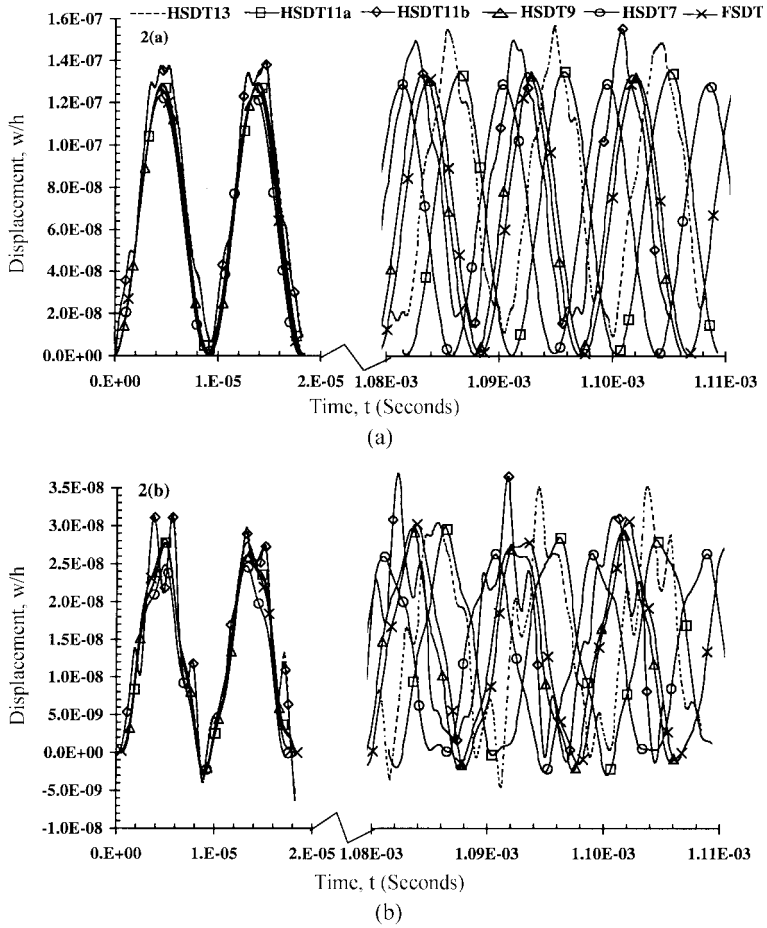

Fig. 2 Transient response of eight-layered unsymmetric cross-ply $(0^o/90^o)_4$ circular cylindrical shell subjected to internal pressure (L/R = 0.5, R/h = 5); (a) w - transverse direction; (b) v - circumferential direction

5. Conclusions

The performance of the present higher-order model over the first- and other standard higher-order models deduced from present theory on the free vibration characteristics, and transient response analyses of thick laminated shells subjected to thermal and mechanical loads has been demonstrated. The inclusion of zig-zag theory along with variable transverse displacement across the thickness, in general, have pronounced effects on the results and they depend on shell parameters and the type of analysis to be carried out in predicting the accurate response characteristics of composite shells.

References

Ali, J.S.M., Bhaskar, K. and Varadan, T.K. (1999), "A new theory for accurate thermal/mechanical flexural analysis of symmetrically laminated plates", *Compos. Struct.*, **45**, 227-232.

Bhaskar, K., Varadan, T.K. and Ali, J.S.M. (1996), "Thermoelastic solutions for orthotropic and anisotropic composite laminates", *Composites: Part B*, **27B**, 415-420.
Bhaskar, K. and Varadan, T.K. (1991), "A higher-order theory for bending analysis of laminated shells of revolution", *Comput. and Struct.*, **40**, 815-819.
Bhimaraddi, A. (1984), "A higher-order theory for free vibration analysis of circular cylindrical shells", *Int. J. Solids Struct.*, **20**, 623-630.
Bhimaraddi, A. (1991), "Free vibration analysis of doubly curved shallow shells on rectangular planform using three-dimensional elasticity theory", *Int. J. Solids Struct.*, **27**, 897-913.
Carrera, E. and Krause, H. (1998), "An investigation of non-linear dynamics of multilayered plates accounting for C_z^0 requirements", *Comput. and Struct.*, **69**, 473-486.
Chang, J.-S. and Huang, Y.-P. (1991), "Geometrically nonlinear static and transiently dynamic behavior of laminated composite plates based on a higher-order displacement field", *Compos. Struct.*, **18**, 327-364.
Cho, K.N., Bert, C.W. and Striz, A.G. (1991), "Free vibrations of laminated rectangular plates analyzed by higher order individual-layer theory", *J. Sound and Vib.*, **145**, 429-442.
Di Sciuva, M. and Icardi, U. (1993), "Discrete-layer models for multilayered anisotropic shells accounting for the interlayers continuity conditions", *Meccanica*, **28**, 281-291.
Ganapathi, M. and Makhecha, D.P. (2001), "Free vibration analysis of multi-layered composite laminates based on an accurate higher-order theory", *Composites, Part B; Engineering*, **32**, 535-543.
He, L.H. (1994), "A linear theory of laminated shells accounting for continuity of displacement and transverse shear stresses at layer interfaces", *Int. J. Solids Struct.*, **31**, 613-627.
Icardi, U. (1998), "Cylindrical bending of laminated cylindrical shells using a modified zig-zag theory", *Struct. Eng. and Mech.*, **5**, 497-516.
Jones, R.M. (1975). *Mechanics of Composite Materials*, McGraw-Hill, New York.
Kant, T. and Swaminathan, K. (2001), "Free vibration of isotropic, orthotropic, and multilayer plates based on higher order refined theories", *J. Sound and Vib.*, **241**, 319-327.
Khdeir, A.A. and Reddy, J.N. (1999), "Free vibrations of laminated composite plates using second-order shear deformation theory", *Comput. and Struct.*, **71**, 617-626.
Kraus, H. (1967). *Thin Elastic shells*, John Wiley, New York.
Lee, K.H., Senthilnathan, N.R., Lim, S.P. and Chow, S.T. (1990), "An improved zigzag model for the bending of laminated composites plates", *Compos. Struct.*, **15**, 137-148.
Lo, K.H., Christensen, R.M. and Wu, E.M. (1977), "A higher-order theory of plate deformation. Part 2: Laminated plates", *J. Appl. Mech.*, ASME, **44**, 669-676.
Makhecha, D.P., Ganapathi, M. and Patel, B.P. (2001), "Dynamic analysis of laminated composite plates subjected to thermal/mechanical loads using an accurate theory", *Compos. Struct.*, **51**, 221-236.
Mallikarjuna. and Kant, T. (1993), "A critical review and some results of recently developed refined theories of fibre reinforced laminated composites and sandwiches", *Compos. Struct.*, **23**, 293-312.
Murukami, H. (1986), "Laminated composite plate theory with improved in-plane responses", *J. Appl. Mech.*, ASME, **53**, 661-666.
Noor, A.K. (1973), "Free vibrations of multilayered composite plates", *AIAA J.*, **11**, 1038-1039.
Noor, A.K. and Burton, W.S. (1990), "Assessment of computational models for multilayered composite shells", *J. Appl. Mech. Rev.*, ASME, **43**, 67-97.
Ossadzow, C., Touratier, M. and Muller, P. (1999), "Deep doubly curved multilayered shell theory", *AIAA J.*, **37**, 100-109.
Prathap, G. (1985), "A C^0 continuos 4-noded cylindrical shell element", *Comput. and Struct.*, **21**, 995-999.
Reddy, J.N. (1990), "A review of refined theories of composite laminates", *Shock and Vibration Digest*, **22**, 3-17.
Shu, X. and Sun, L. (1994), "An improved simple higher order theory for a laminated composite plates", *Comput. and Struct.*, **50**, 231-236.
Tenneti, R. and Chandrashekhara, K. (1994), "Nonlinear thermal dynamic analysis of graphite/aluminum composite plates", *AIAA J.*, **32**, 1931-1933.
Xavier, P.B., Lee, K.H. and Chew, C.H. (1993), "An improved zig-zag model for the bending of laminated composite shells", *Compos. Struct.*, **26**, 123-138.
Ye, J.Q. and Soldatos, K.P. (1997), "Three-dimensional vibrations of cross-ply laminated hollow cylinders with

clamped edge boundaries", *J. Vibration and Acoustics*, ASME, **119**, 317-323.
Zienkiewicz, O.C. (1971). *Finite Element Methods in Engineering Science*, McGraw-Hill, London.

Appendix A

The various submatrices involved in Eq. (5) are

$$[Z_1] = \begin{bmatrix} \frac{1}{1+z/R_1} & 0 & 0 & 0 & 0 \\ 0 & \frac{1}{1+z/R_2} & 0 & 0 & 0 \\ 0 & 0 & 1 & 0 & 0 \\ 0 & 0 & 0 & \frac{1}{1+z/R_1} & \frac{1}{1+z/R_2} \end{bmatrix}; [Z_2] = z[Z_1];$$

$$[Z_3] = \begin{bmatrix} \frac{z^2}{1+z/R_1} & 0 & 0 & 0 \\ 0 & \frac{z^2}{1+z/R_2} & 0 & 0 \\ 0 & 0 & 0 & 0 \\ 0 & 0 & \frac{z^2}{1+z/R_1} & \frac{z^2}{1+z/R_2} \end{bmatrix}; [Z_4] = z[Z_3];$$

$$[Z_5] = \begin{bmatrix} \frac{S^k}{1+z/R_1} & 0 & 0 & 0 \\ 0 & \frac{S^k}{1+z/R_2} & 0 & 0 \\ 0 & 0 & 0 & 0 \\ 0 & 0 & \frac{S^k}{1+z/R_1} & \frac{S^k}{1+z/R_2} \end{bmatrix}; [Z_6] = \begin{bmatrix} 1 & 0 \\ 0 & 1 \end{bmatrix}; [Z_7] = z[Z_6]; [Z_8] = z^2[Z_6]; [Z_9] = S^k_{,z}[Z_6];$$

$$[Z_{10}] = \begin{bmatrix} \frac{1}{1+z/R_1} & 0 \\ 0 & \frac{1}{1+z/R_2} \end{bmatrix}; [Z_{11}] = z[Z_{10}]; [Z_{12}] = z^2[Z_{10}]; [Z_{13}] = z^3[Z_{10}]; [Z_{14}] = S^k[Z_{10}] \qquad \text{(A1)}$$

$$\{\varepsilon_1\} = \begin{Bmatrix} \frac{\partial u_0}{\partial x} + \frac{w_0}{R_1} \\ \frac{\partial v_0}{\partial y} + \frac{u_0}{r}\cos\phi + \frac{w_0}{r}\sin\phi \\ w_1 \\ \frac{\partial v_0}{\partial x} \\ \frac{\partial u_0}{\partial y} - \frac{v_0}{r}\cos\phi \end{Bmatrix}; \quad \{\varepsilon_2\} = \begin{Bmatrix} \frac{\partial \theta_x}{\partial x} + \frac{w_1}{R_1} \\ \frac{\partial \theta_y}{\partial y} + \frac{\theta_x}{r}\cos\phi + \frac{w_1}{r}\sin\phi \\ 2\Gamma \\ \frac{\partial \theta_y}{\partial x} \\ \frac{\partial \theta_x}{\partial y} - \frac{\theta_y}{r}\cos\phi \end{Bmatrix};$$

$$\{\varepsilon_3\} = \begin{Bmatrix} \dfrac{\partial \beta_x}{\partial x} + \dfrac{\Gamma}{R_1} \\ \dfrac{\partial \beta_y}{\partial y} + \dfrac{\beta_x}{r}\cos\phi + \dfrac{\Gamma}{r}\sin\phi \\ \dfrac{\partial \beta_y}{\partial x} \\ \dfrac{\partial \beta_x}{\partial y} - \dfrac{\beta_y}{r}\cos\phi \end{Bmatrix}; \quad \{\varepsilon_4\} = \begin{Bmatrix} \dfrac{\partial \phi_x}{\partial x} \\ \dfrac{\partial \phi_y}{\partial y} + \dfrac{\phi_x}{r}\cos\phi \\ \dfrac{\partial \phi_y}{\partial x} \\ \dfrac{\partial \phi_x}{\partial y} - \dfrac{\phi_y}{r}\cos\phi \end{Bmatrix}; \quad \{\varepsilon_5\} = \begin{Bmatrix} \dfrac{\partial \psi_x}{\partial x} \\ \dfrac{\partial \psi_y}{\partial y} + \dfrac{\psi_x}{r}\cos\phi \\ \dfrac{\partial \psi_y}{\partial x} \\ \dfrac{\partial \psi_x}{\partial y} - \dfrac{\psi_y}{r}\cos\phi \end{Bmatrix} \tag{A2}$$

$$\{\varepsilon_6\} = \begin{Bmatrix} \theta_x \\ \theta_y \end{Bmatrix}; \quad \{\varepsilon_7\} = \begin{Bmatrix} 2\beta_x \\ 2\beta_y \end{Bmatrix}; \quad \{\varepsilon_8\} = \begin{Bmatrix} 3\phi_x \\ 3\phi_y \end{Bmatrix}; \quad \{\varepsilon_9\} = \begin{Bmatrix} \psi_x \\ \psi_y \end{Bmatrix}; \quad \{\varepsilon_{10}\} = \begin{Bmatrix} \dfrac{\partial w_0}{\partial x} - \dfrac{u_0}{R_1} \\ \dfrac{\partial w_0}{\partial y} - \dfrac{v_0}{r}\sin\phi \end{Bmatrix};$$

$$\{\varepsilon_{11}\} = \begin{Bmatrix} \dfrac{\partial w_1}{\partial x} - \dfrac{\theta_x}{R_1} \\ \dfrac{\partial w_1}{\partial y} - \dfrac{\theta_y}{r}\sin\phi \end{Bmatrix}; \quad \{\varepsilon_{12}\} = \begin{Bmatrix} \dfrac{\partial \Gamma}{\partial x} - \dfrac{\beta_x}{R_1} \\ \dfrac{\partial \Gamma}{\partial y} - \dfrac{\beta_y}{r}\sin\phi \end{Bmatrix}; \quad \{\varepsilon_{13}\} = \begin{Bmatrix} -\dfrac{\phi_x}{R_1} \\ -\dfrac{\phi_y}{r}\sin\phi \end{Bmatrix}; \quad \{\varepsilon_{14}\} = \begin{Bmatrix} -\dfrac{\psi_x}{R_1} \\ -\dfrac{\psi_y}{r}\sin\phi \end{Bmatrix} \tag{A3}$$

O_1, O_2 and O_3 are null matrices of size 4×2, 2×5, and 2×4, respectively.